Title

Lysosome inhibition sensitizes pancreatic cancer to replication stress by aspartate depletion

Permalink

https://escholarship.org/uc/item/58d3s4xd

Journal

Proceedings of the National Academy of Sciences of the United States of America, 116(14)

ISSN

0027-8424

Authors

Elliott, Irmina A
Dann, Amanda M
Xu, Shili
et al.

Publication Date

2019-04-02

DOI

10.1073/pnas.1812410116

Peer reviewed

Lysosome inhibition sensitizes pancreatic cancer to replication stress by aspartate depletion

Irmina A. Elliott[a,1], Amanda M. Dann[a,1], Shili Xu[a,b,c,1], Stephanie S. Kim[a], Evan R. Abt[b,c], Woosuk Kim[b,c], Soumya Poddar[b,c], Alexandra Moore[a], Lei Zhou[a,d], Jennifer L. Williams[e], Joseph R. Capri[b,c], Razmik Ghukasyan[a], Cynthia Matsumura[a], D. Andrew Tucker[a,f], Wesley R. Armstrong[b,c], Anthony E. Cabebe[b,c], Nanping Wu[a], Luyi Li[a], Thuc M. Le[b,c], Caius G. Radu[a,b,c,f,g,2], and Timothy R. Donahue[a,b,c,f,g,2]

[a]Department of Surgery, University of California, Los Angeles, CA 90095; [b]Department of Molecular and Medical Pharmacology, University of California, Los Angeles, CA 90095; [c]Ahmanson Translational Imaging Division, University of California, Los Angeles, CA 90095; [d]Department of Pancreatic and Thyroidal Surgery, Shengjing Hospital, China Medical University, Shenyang 110003, China; [e]Department of Surgery, Harbor–UCLA Medical Center, Torrance, CA 90502; [f]David Geffen School of Medicine, University of California, Los Angeles, CA 90095; and [g]Jonsson Comprehensive Cancer Center, University of California, Los Angeles, CA 90095

Functional lysosomes mediate autophagy and macropinocytosis for nutrient acquisition. Pancreatic ductal adenocarcinoma (PDAC) tumors exhibit high basal lysosomal activity, and inhibition of lysosome function suppresses PDAC cell proliferation and tumor growth. However, the codependencies induced by lysosomal inhibition in PDAC have not been systematically explored. We performed a comprehensive pharmacological inhibition screen of the protein kinome and found that replication stress response (RSR) inhibitors were synthetically lethal with chloroquine (CQ) in PDAC cells. CQ treatment reduced de novo nucleotide biosynthesis and induced replication stress. We found that CQ treatment caused mitochondrial dysfunction and depletion of aspartate, an essential precursor for de novo nucleotide synthesis, as an underlying mechanism. Supplementation with aspartate partially rescued the phenotypes induced by CQ. The synergy of CQ and the RSR inhibitor VE-822 was comprehensively validated in both 2D and 3D cultures of PDAC cell lines, a heterotypic spheroid culture with cancer-associated fibroblasts, and in vivo xenograft and syngeneic PDAC mouse models. These results indicate a codependency on functional lysosomes and RSR in PDAC and support the translational potential of the combination of CQ and RSR inhibitors.

lysosome | autophagy | replication stress | pancreatic cancer | nucleotide metabolism

Pancreatic ductal adenocarcinoma (PDAC) is the fourth leading cause of cancer-related death in the United States, and its incidence is increasing (1). PDAC carries a 5-y survival of less than 10%, as it is often diagnosed at a late stage and is widely refractory to available therapies. This lack of effective treatment options suggests an incomplete understanding of the biologic complexity of PDAC and mechanisms of therapeutic resistance.

PDAC tumors are hypoperfused, resulting in poor nutrient delivery (2). To exist in this hostile microenvironment, PDAC cells rely on intracellular and extracellular scavenging pathways to acquire metabolic substrates for growth. Autophagy, a self-degradative mechanism employed to recycle damaged cytosolic proteins and organelles, and macropinocytosis, the process of uptaking bulk extracellular material, are up-regulated in PDAC (3–6). As the final step of both autophagy and macropinocytosis, autophagic and endocytic cargo fuse with the lysosome, where macromolecules are degraded and substrates for metabolism are released (3, 4, 7). Inhibition of these pathways suppresses PDAC tumor growth and prolongs survival in animal models (4, 6, 8). Additionally, engaging autophagic programs confers resistance to chemoradiation in PDAC cells (9–11), and high levels of autophagy markers are correlated with worse survival in resected PDAC patients (12).

The study of lysosomal function often focuses on proteolysis, which degrades misfolded proteins and damaged organelles (13,

14). However, lysosomal degradation pathways also play a critical role in lipid (15–17) and nucleic acid metabolism. The recycling of nucleic acid species by lysosomes maintains genomic integrity and regulates immune sensing of pathogen or aberrant self-DNA and RNA (18). Lysosomes also supply metabolic substrates to maintain nucleotide pools in cancer cells (14).

DNA replication and cancer cell proliferation require a sufficient supply of nucleotides. Two convergent pathways exist for nucleotide synthesis: (*i*) the de novo pathway, which synthesizes nucleotides from glucose and amino acid precursors, and (*ii*) the nucleoside salvage pathway (19, 20). Cotargeting these pathways inhibits cancer progression (21, 22). In response to nucleotide insufficiency, cells engage the replication stress response (RSR) pathway, a signaling cascade mediated by ataxia telangiectasia and Rad3-related protein (ATR) and its downstream checkpoint kinases CHEK1 and WEE1. Activation of this pathway coordinates cell cycle checkpoint activation, replication fork stabilization, restoration of nucleotide pools, and, ultimately, firing of new replication origins. The ATR inhibitor VE-822, currently in phase I/II clinical trials for multiple cancer types, sensitizes cancer cells to inhibition of nucleotide biosynthesis (23).

Significance

Pancreatic cancer is notoriously treatment resistant. These tumors rely on lysosome-dependent recycling pathways to generate substrates for metabolism, which are inhibited by chloroquine (CQ) and its derivatives. However, clinical efficacy of CQ as a monotherapy or combined with standard-of-care regimens has been limited. Using an unbiased kinome screen, we identify replication stress as an induced vulnerability of CQ due to impaired de novo nucleotide biosynthesis and find that combination treatment with CQ and a replication stress response inhibitor is synthetically lethal in pancreatic cancer.

Extensively used in patients, chloroquine (CQ) and its derivatives deacidify lysosomes, thus inhibiting autophagy (24). These agents have been investigated in multiple cancers but show limited efficacy in PDAC as monotherapy or in combination with standard-of-care therapies (25–27). In this study, we performed an unbiased kinome inhibition screen to identify previously unexplored vulnerabilities of CQ-treated PDAC cells and found the replication stress pathway to be the most prominent codependency. We validated the synthetic lethality of CQ and the RSR inhibitor VE-822 in multiple in vitro and in vivo PDAC models. Mechanistically, we found that lysosome inhibition led to mitochondrial dysfunction and decreased aspartate, resulting in decreased de novo nucleotide synthesis, thereby inducing replication stress.

Results

Kinase Inhibitor Screen Identifies the Replication Stress Pathway as a Codependency of Impaired Lysosome Function.

A kinase inhibitor screen identified the RSR–ATR/CHEK1 pathway as the most prominent codependency of CQ-treated cells (Fig. 1A). All ATR and CHEK1 inhibitors scored positively (Dataset S1). The synergy between CQ and the RSR inhibitors was validated in a secondary assay (SI Appendix, Fig. S1A). Among these RSR inhibitors, ATR inhibitor VE-822 (also known as VX-970 or Berzosertib) was selected for further analysis due to its translational potential; VE-822 has favorable pharmacodynamics and tolerability in animal models (23, 28). The CQ/VE-822 synergy was confirmed using the combination index (SI Appendix, Fig. S1B) and in a panel of PDAC cell lines in both 2D monolayer and 3D spheroid cultures (Fig. 1B). The synthetic lethality of CQ and VE-822 was supported by the synergistic induction of pH2A.X, a marker of DNA damage (Fig. 1C). In addition, CQ and VE-822 showed synergy in a majority of human PDAC cell lines and primary cultures (XWR200, A13A, and A2.1) (Fig. 1D).

Lysosome Inhibition Induces Replication Stress.

We hypothesized synergy between CQ and RSR inhibitors occurred because
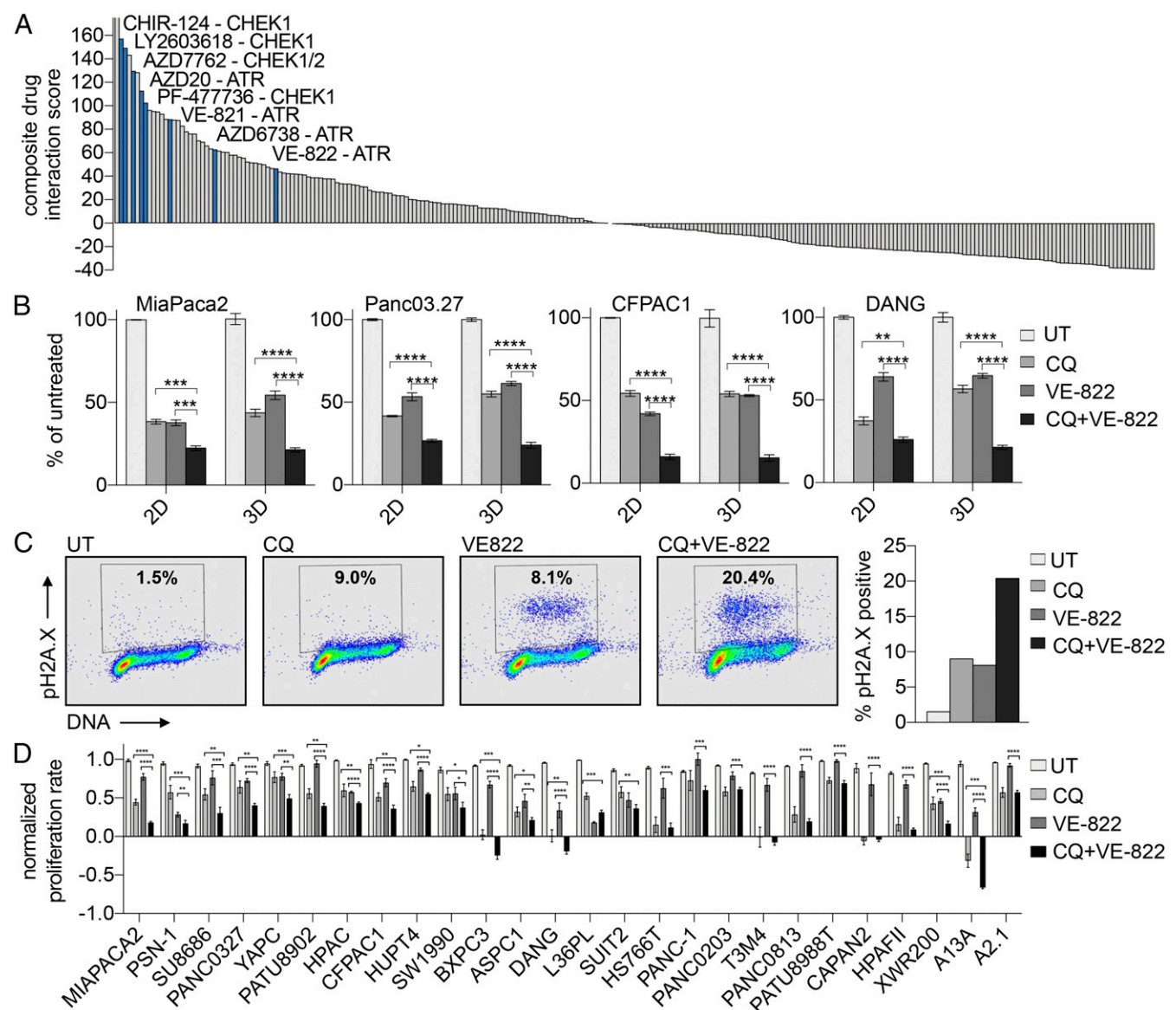

Fig. 1. RSR inhibitors synergize with CQ to inhibit cell growth. (A) Composite drug interaction score of CQ and 430 kinase inhibitors screened for growth inhibition in MiaPaca2 cells (n = 2). (B) Viability of PDAC cells in 2D and 3D cultures ± CQ ± VE-822 for 72 h (n = 3). (C) Flow cytometry analyses of DNA content and DNA damage marker pH2A.X in MiaPaca2 cells treated ± CQ ± VE-822 for 24 h (n = 2). (D) The antiproliferation effect of CQ/VE-822 combination in a panel of human PDAC cell lines and primary PDAC cultures. UT, untreated. CQ: 20 μM; VE-822: 500 nM. **P < 0.01, ***P < 0.001, ****P < 0.0001.
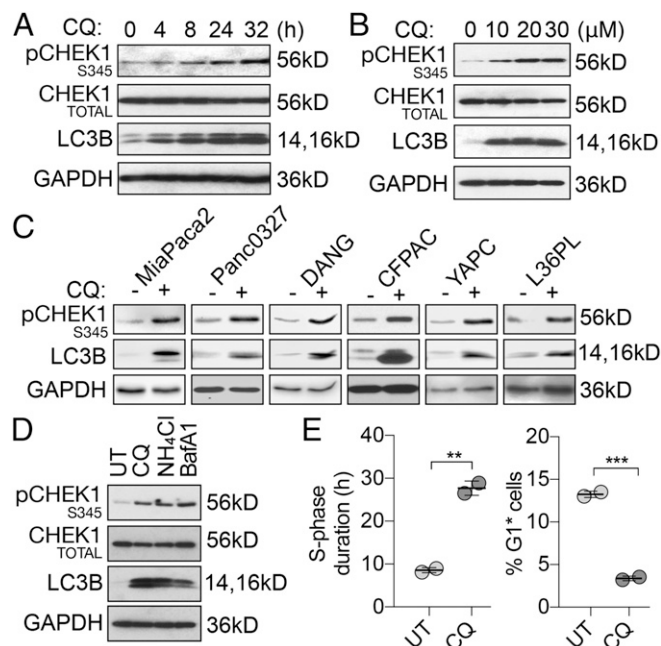
Fig. 2. Lysosomal inhibitors induce replication stress. (*A*) Time course effects of 20 μM of CQ on replication stress marker pCHEK1-S345 and on autophagy marker LC3B in MiaPaca2 cells. (*B*) Dose–response effects of 24-h CQ treatment on pCHEK1-S345 and LC3B in MiaPaca2 cells. (*C*) Effect of CQ treatment for 24 h on pCHEK1-S345 and LC3B in a panel of PDAC cell lines. (*D*) Effects of 24-h treatment with lysosome inhibitors on pCHEK1-S345 and LC3B in MiaPaca2. (*E*) Measurements of S-phase duration and G1 cell percentage by EdU pulse–chase flow cytometry analysis. All immunoblots are representative of at least two independent experiments. CQ: 20 μM unless otherwise indicated; NH4Cl: 10 mM; BafA1: 10 nM. **$P < 0.01$, ***$P < 0.001$.

lysosomal inhibition increased replication stress. We observed induction of pCHEK1 (S345), a marker of RSR, by 8 h after CQ exposure in MiaPaca2 cells, which continued to increase up to 32 h. Accumulation of LC3B confirmed CQ inhibition of autophagolysosome maturation (Fig. 2*A*). Increasing pCHEK1 induction was also noted with increasing doses of CQ (Fig. 2*B*). These findings were consistent across a panel of PDAC lines (Fig. 2*C*). Similar to CQ, other lysosome inhibitors, including ammonium chloride (NH4Cl) and bafilomycin A1 (BafA1), induced pCHEK1 (Fig. 2*D*), indicating RSR activation is an on-target effect of lysosome inhibition. These lysosomal inhibitors synergistically inhibited PDAC cell growth when combined with VE-822 (*SI Appendix*, Fig. S2*A*). A 5-ethynyl-2-deoxyuridine (EdU) pulse–chase assay to profile cell cycle kinetics was used orthogonally to examine replication stress, which occurs at stalled replication forks and prolongs cell cycle S phase. Consistent with pCHEK1 induction, CQ significantly prolonged S-phase duration and resulted in fewer labeled cells reentering the G1 phase of the cell cycle (G1*) (Fig. 2*E* and *SI Appendix*, Fig. S2*B*).

Lysosome Inhibition Impairs de Novo Nucleotide Biosynthesis. Insufficiency of essential replication factors, including replication machinery and deoxyribonucleotides (dNTPs), is a known cause of stalled replication forks and replication stress (29–31). To investigate the effect of CQ on dNTP availability, we used a previously described liquid chromatography (LC)-mass spectrometry (MS)/MS-multiple reaction monitoring (MRM) method to measure heavy-isotope labeled nucleotides, in the form of both free metabolites and hydrolyzed nucleic acids species (DNA/RNA), from cells cultured with [$^{13}C_6$]glucose (23). This method determines the contribution of nucleotides to free dNTP and ribonucleotide (rNTP) pools and incorporation into newly synthesized RNA and DNA. CQ decreased all four labeled dNTP pools

(dCTP, TTP, dATP, and dGTP) (Fig. 3*A*) and the percentage labeling of DNA across all four bases (Fig. 3*B*). CQ appeared to selectively inhibit de novo dNTP biosynthesis, as unlabeled dNTP pools remained unaffected or increased in CQ-treated cells (*SI Appendix*, Fig. S3). De novo produced dNTPs are more readily incorporated into DNA than those produced by the salvage pathway (unlabeled dNTPs) (21, 32), suggesting that it is the decrease specifically in de novo dNTP biosynthesis that causes replication stress in CQ-treated cells.

To further investigate the source of the defect in de novo dNTP synthesis, we assessed the impact of CQ on de novo synthesized ribonucleotide pools. Impaired de novo dNTP biosynthesis may be caused by a shortage of substrates for nucleotide synthesis (e.g., glucose, amino acids) or by ribonucleotide reductase (RNR) inhibition, preventing RNR reduction of ribonucleotide diphosphates to deoxyribonucleotide diphosphates, the rate-limiting step in de novo dNTP production. MiaPaca2 cells cultured with [$^{13}C_6$]glucose ± CQ were analyzed for labeled NTP pools and their incorporation into RNA. We observed no significant changes in NTP pools with CQ treatment but a decrease in labeled RNA (Fig. 3 *C* and *D*), suggesting an overall decrease in de novo nucleotide synthesis. These results indicate CQ treatment impairs de novo synthesis of both dNTPs and NTPs, rather than a defect in conversion of ribo- to deoxyribonucleotides by RNR.

Lysosome Inhibition Depletes Aspartate. In de novo nucleotide biosynthesis, the amino acid precursors Asp, Gln, Gly, and Ser are utilized for purine biosynthesis, while only Asp and Gln are required for pyrimidine ribonucleotide synthesis. CQ treatment significantly decreased intracellular Asp levels while increasing Gln, Gly, and Ser levels (Fig. 4*A*). As non-Gln amino acids are important sources of carbon and nitrogen biomass in cancer cells (33), we further assess if CQ treatment resulted in a global decrease in non-Gln amino acids and thus a general decrease in
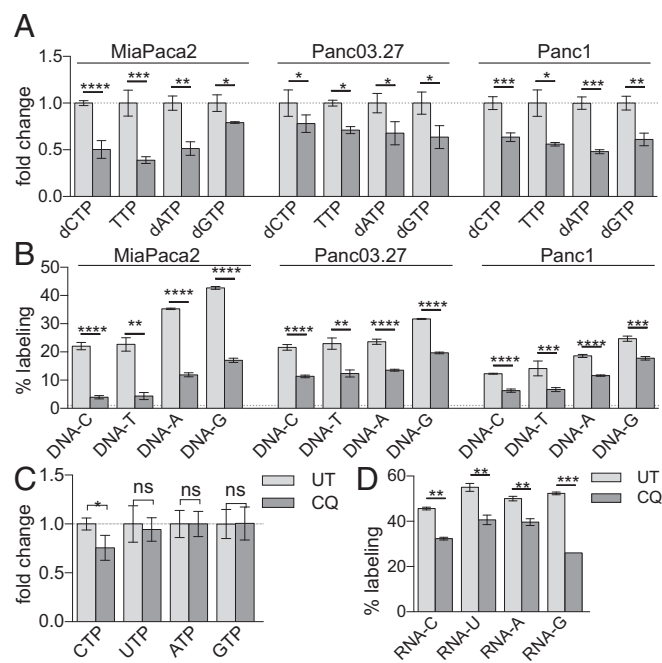

Fig. 3. CQ treatment impairs de novo nucleotide biosynthesis. LC-MS/MS-MRM analysis of (*A*) relative levels of [$^{13}C_6$]glucose-labeled dNTPs and (*B*) percentage of [$^{13}C_6$]glucose labeling of the four DNA bases (DNA-C, DNA-T, DNA-A, DNA-G) in PDAC cells ± CQ ($n = 3$). (*C*) Relative levels of [$^{13}C_6$]glucose-labeled NTPs and (*D*) percentage of [$^{13}C_6$]glucose labeling of RNA in MiaPaca2 ($n = 3$). CQ: 20 μM; 24-h treatment. *$P < 0.05$, **$P < 0.01$, ***$P < 0.001$, ****$P < 0.0001$; ns, not significant.
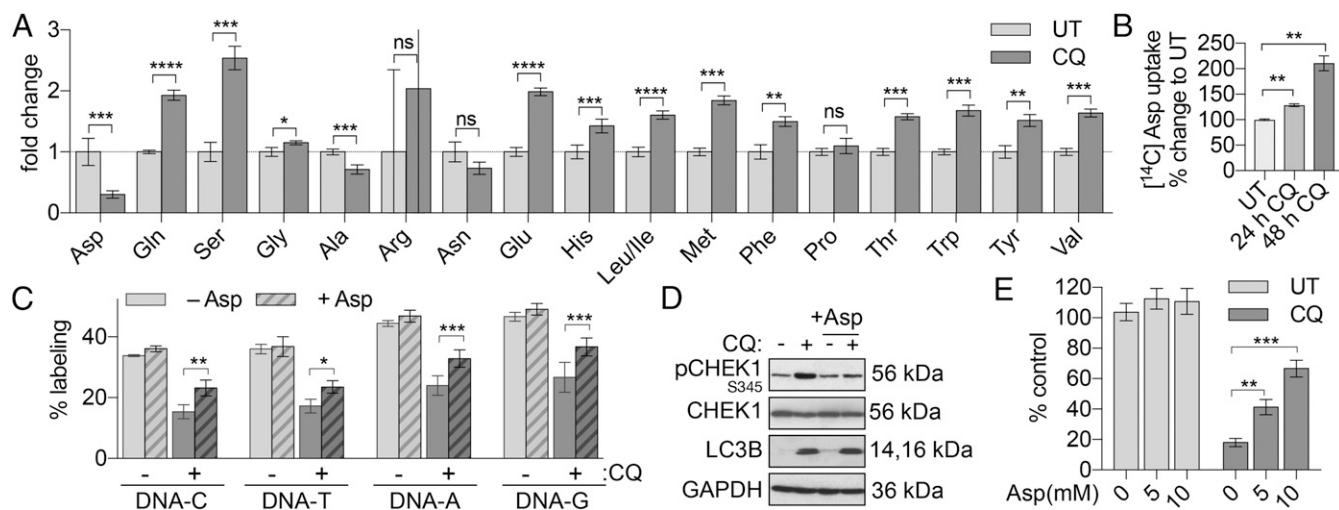
Fig. 4. Asp depletion by CQ impairs de novo nucleotide biosynthesis, induces RSR, and inhibits PDAC cell proliferation. (*A*) Relative amino acid levels measured by LC-MS in MiaPaca2 cells ± CQ for 48 h (*n* = 3). (*B*) CQ treatment increased [^{14}C]Asp uptake by MiaPaca2 cells. (*C*) [$^{13}C_6$]glucose-labeled DNA bases (DNA-C, DNA-T, DNA-A, DNA-G) measured by LC-MS/MS-MRM in MiaPaca2 cells ± CQ ± Asp for 72 h (*n* = 3). (*D*) pCHEK1-S345 and LC3B levels in MiaPaca2 cells ± CQ ± Asp for 24 h. (*E*) Viability of MiaPaca2 cells ± CQ ± Asp for 72 h (*n* = 3). CQ: 20 μM; Asp: 10 mM. *$P < 0.05$, **$P < 0.01$, ***$P < 0.001$, ****$P < 0.0001$; ns, not significant.

carbon and nitrogen sources. Other than Asp, Ala was the only amino acid that exhibited a significant, but smaller, decrease with CQ treatment (Fig. 4*A* and Dataset S2). The reduction of Asp was confirmed using an orthogonal Asp assay (*SI Appendix*, Fig. S4*A*). In addition, CQ treatment increased Asp uptake, suggesting increased Asp demand (Fig. 4*B*). These results imply that Asp is the major amino acid affected by CQ and that Asp is the limiting substrate for de novo nucleotide biosynthesis in the setting of lysosomal inhibition.

We then performed rescue experiments with Asp supplementation to implicate Asp deficiency as a cause of CQ-induced nucleotide insufficiency and replication stress. Asp supplementation rescued Asp levels (*SI Appendix*, Fig. S4*B*), partially restored the decrease in DNA labeling with CQ treatment in all four nucleobases (Fig. 4*C*), and prevented CQ-induced replication stress (Fig. 4*D*). Asp supplementation partially rescued CQ- and NH₄Cl-induced growth inhibition in a dose-dependent manner (Fig. 4*E* and *SI Appendix*, Fig. S4 *C* and *D*) and CQ-induced DNA damage (*SI Appendix*, Fig. S4*E*). The growth rescue effect of Asp exceeded those of dNTP substrates (de novo substrates Gln, Ser, and Gly and salvage substrates rNs and dNs) and other amino acids (*SI Appendix*, Fig. S4 *F* and *G*).

We hypothesized that CQ treatment could cause mitochondrial dysfunction, resulting in decreased electronic transportation chain (ETC) activity and therefore inhibit Asp biosynthesis (34). To test this hypothesis, we examined mitochondrial membrane potential, a marker of mitochondrial damage (35), in PDAC cells treated with CQ. Chronic, but not acute, treatment with CQ increased mitochondrial membrane potential (Fig. 5*A*), indicating accumulation of damaged mitochondria (35). In addition, CQ reduced ETC activity (Fig. 5*B*), an important function of mitochondria to enable Asp synthesis (34). Pyruvate supplement, which supports Asp synthesis when ETC activity is reduced (35), partially rescued CQ-induced Asp depletion (Fig. 5*C*) and inhibition of PDAC cell proliferation (Fig. 5*D*).

Lysosome Inhibition Synergizes with RSR Inhibitors in Complex, Organotypic in Vitro Models and in Vivo. PDAC tumors are characterized by a dense stroma, primarily composed of fibroblasts and extracellular matrix (36). These cancer-associated fibroblasts (CAFs) support cancer cell proliferation and confer resistance to chemoradiation (37, 38). Therefore, we used a 3D organotypic MiaPaca2/CAF coculture model to assess the efficacy of CQ/VE-822 in stroma-rich PDAC tumors. In contrast to monoculture, the growth of cocultured spheroids was not affected by VE-822. CQ treatment resulted in similar growth inhibition in these

cocultures as in a 2D monoculture, and the combination showed substantial synergy (Fig. 6 *A* and *B*).

In an in vivo PDAC model, the combination of CQ and VE-822 synergistically slowed the growth of xenograft MiaPaca2 tumors (Fig. 6*C*, 32% reduction in size at final time point). Overexpression of the Asp transporter SLC1A3 (39) increased Asp levels and was protective against CQ- and CQ/VE-822–induced
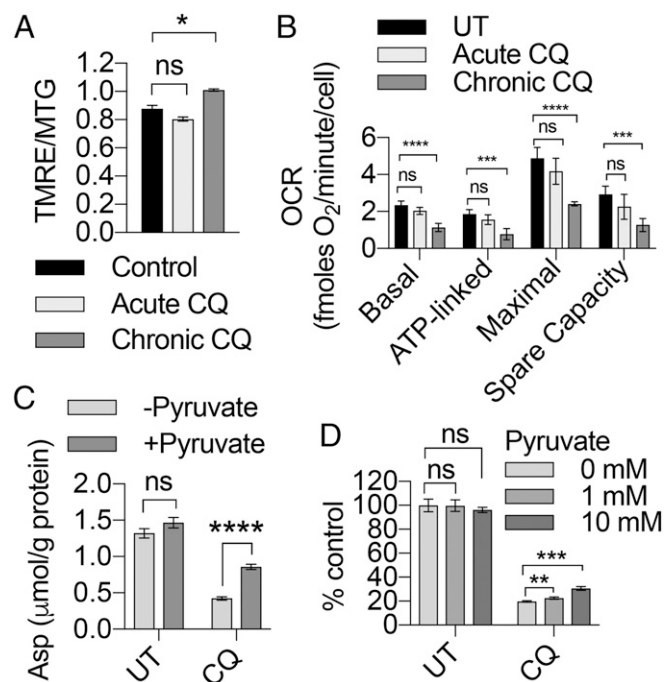

Fig. 5. CQ causes mitochondrial dysfunction. (*A*) Chronic CQ treatment induces mitochondrial membrane potential heterogeneity. MTG, MitoTracker Green; TMRE, tetramethylrhodamine ethyl ester. (*B*) Chronic CQ treatment reduced mitochondrial respiration. OCR, oxygen consumption rate. (*C*) Pyruvate supplementation (1 mM) rescued CQ-induced Asp reduction in MiaPaca2 cells. (*D*) Pyruvate supplementation rescued CQ-induced proliferation inhibition in MiaPaca2 cells. CQ: 20 μM; acute: 2 h; chronic: 24 h. *$P < 0.05$, **$P < 0.01$, ***$P < 0.001$, ****$P < 0.0001$; ns, not significant.

decreases in Asp levels (*SI Appendix*, Fig. S5 *A–C*). In vivo, overexpression of SLC1A3 in MiaPaca2 xenograft tumors rescued the growth inhibition caused by CQ/VE-822 (*SI Appendix*, Fig. S5*D*). The CQ/VE-822 combination significantly decreased the proliferation marker Ki67 and increased the frequencies of DNA damage marker pH2A.X-positive cells and apoptosis markers cleaved caspase-3– and cleaved PARP-positive cells in MiaPaca2 tumors (Fig. 6*D*). Similar to our observations in human PDAC cells, CQ and VE-822 synergistically inhibited the proliferation of cultured murine PDAC KPC cells (*SI Appendix*, Fig. S6*A*), and this was partially rescued by Asp supplementation (*SI Appendix*, Fig. S6*B*). In an in vivo syngeneic KPC PDAC tumor model, the combination of CQ and VE-822 significantly slowed tumor growth (Fig. 6*E*) and induced DNA damage, as indicated by pH2A.X staining (Fig. 6*F*). These results suggest the combination of CQ and VE-822 may represent a promising therapeutic strategy in PDAC.

Discussion

PDAC tumors rely on intracellular and extracellular nutrient scavenging to sustain growth. Disabling these pathways with inhibitors of lysosome function has been effective in preclinical models (4), but this strategy has shown limited efficacy in clinical trials (26). Understanding how tumor cells respond to lysosomal inhibitors is required to leverage these agents as PDAC therapeutics. Here, we show that inhibition of lysosomal function in PDAC cells depletes Asp required for de novo nucleotide biosynthesis. This results in deoxyribonucleotide insufficiency and an increased reliance on the RSR pathway. Further, combination treatment with CQ and a RSR inhibitor is synthetically lethal in in vitro and in vivo PDAC models.

Deletion of autophagy genes decreases nucleotide pools in *Ras*-driven cancers (14). Guo et al. (14) found that nutrient deprivation increases catabolism of ribonucleotides to generate ribose phosphate to maintain energy charge, thereby increasing

reliance on autophagy-generated Gln for nucleotide biosynthesis. Lung cancer cells deficient of ATG7 were less efficient at Gln recycling and exhibited more pronounced ribonucleotide depletion than their autophagy-proficient counterparts under starvation. Perera et al. (3) found silencing TFE genes, transcription factors regulating lysosomal biogenesis (40), decreased Gln and the pyrimidine nucleoside cytidine. However, the role of lysosome in maintaining deoxyribonucleotide pools to sustain DNA replication and mitigate replication stress in PDAC has not been systematically investigated.

Our data support a model in which CQ treatment critically depletes Asp in PDAC cells, restricting de novo dNTP synthesis. Previous reports addressing how lysosome or autophagy inhibition influences Asp levels are conflicting. Guo et al. (14) showed that ATG7-null mouse lung cancer cells exhibited impaired ability to recycle Asp, but viability of autophagy-deficient cells was rescued with Gln, not Asp, supplementation. This contrasts our findings in which Asp, but not Gln, was decreased following lysosomal inhibition and growth inhibition by CQ was most efficiently rescued with Asp supplementation. Zhang et al. (41) found autophagy-proficient and -deficient cells had equivalent concentrations of Asp. These differences may be due to the unique Gln metabolism pathway in PDAC (42). In addition, Zhang et al. (41) found the concentrations of most amino acids in autophagy-deficient cells increased under starvation conditions due to up-regulation of cell surface transporters. Given we observed an increase in the majority of amino acids following CQ treatment, a similar mechanism may occur following lysosomal inhibition. Others have shown that acute lysosomal inhibition does not significantly change whole cell levels of Asp but increases its lysosomal concentration (43). These observations suggest cellular responses to genetic inhibition of autophagy may not phenocopy those of pharmacologic lysosomal inhibition and that the role of lysosome in amino acid pool maintenance may be cell- and environment context-specific. Previous work identified
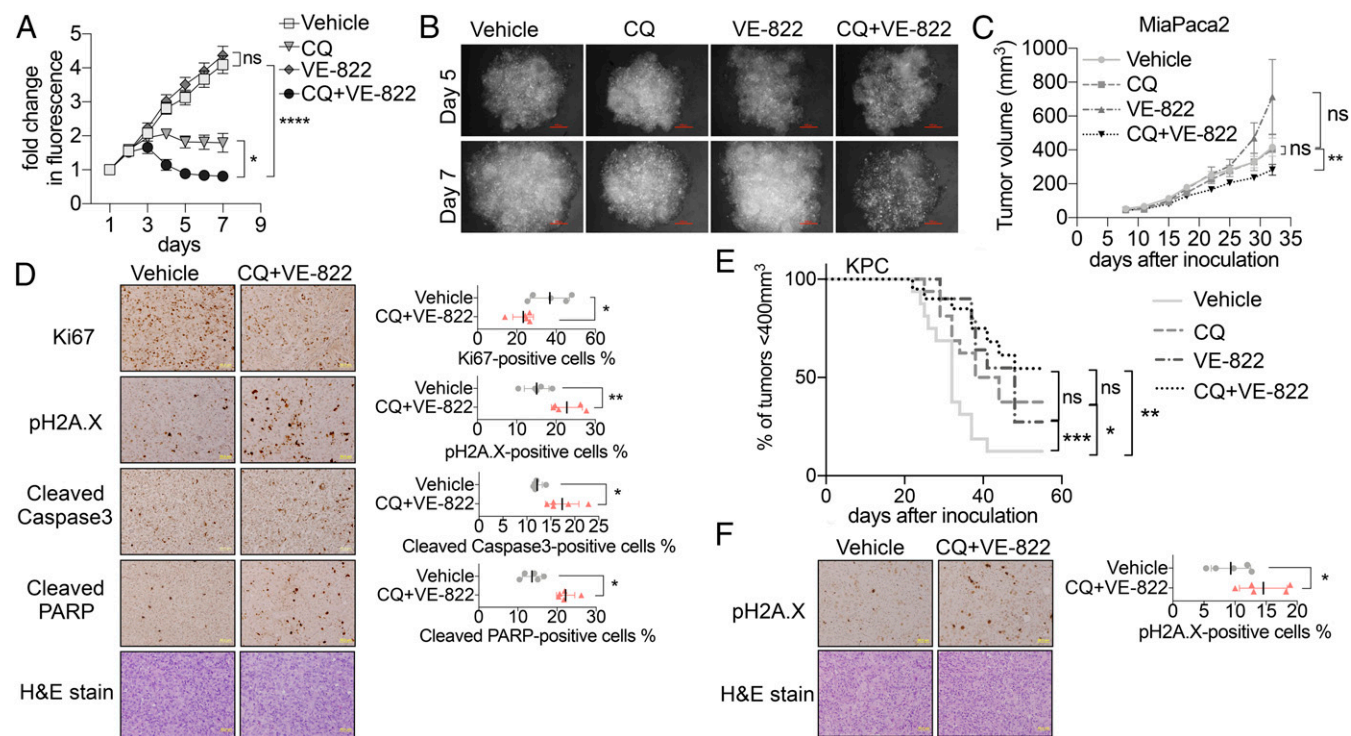

Fig. 6. CQ and VE-822 synergistically inhibit tumor cell growth in organotypic in vitro and in vivo PDAC models. (*A*) Viability of MiaPaca2-GFP cells in CAF coculture ± CQ ± VE-822 (*n* = 3). (*B*) Representative fluorescence images of *A*. (Scale bar, 0.05 μm.) (*C*) Xenograft MiaPaca2 tumor growth ± CQ ± VE-822. (*D*) IHC staining of indicated markers in MiaPaca2 tumors after 5-d vehicle or CQ/VE-822 treatments. (*E*) Kaplan–Meier curves of tumors in syngeneic KPC mouse models ± CQ ± VE-822. (*F*) IHC staining of indicated markers in KPC tumors with 5-d vehicle or CQ/VE-822 treatments. *$P < 0.05$, **$P < 0.01$, ***$P < 0.001$.

a synergistic interaction between CQ and inhibitors of CHEK1 in targeting colon and osteosarcoma cancer cells (44). However, rather than CQ causing nucleotide insufficiency, the synergy was attributed to the fact that genetic autophagy inhibition has been shown to enhance proteasomal degradation of CHEK1 (45) and thereby increase the potency of CHEK1 inhibitors. In our models, pharmacologic lysosome inhibition did not decrease total CHEK1 protein levels, suggesting CQ-induced dNTP pool depletion, leading to increased replication stress, is the primary mechanism underlying this synergy. Our findings suggest the addition of RSR inhibitors could improve the efficacy of lysosomal inhibitors in PDAC and represent a rationally designed drug combination in this notoriously treatment resistant disease.

Experimental Procedures

Cell Culture. MiaPaca2, CFPAC1, Panc03.27, and Panc1 were purchased from American Type Culture Collection. DANG, L3.6pl, YAPC, and MiaPaca2-GFP were provided by Dr. David Dawson, University of California, Los Angeles (UCLA). KPC cells were provided by Dr. Guido Eibl, UCLA. Primary human cancer-associated fibroblasts were isolated from surgical PDAC specimens by an outgrowth method (46) and characterized (47). The primary PDAC model XWR200 was developed from a patient at UCLA. Primary PDAC models A2.1 and A13A were provided by Dr. Christine A. Iacobuzio-Donahue, Memorial Sloan Kettering Cancer Center, New York.

[14C]Asp Uptake Assay. [14C]Asp uptake assay was performed as described (39). MiaPaca2 cells were pretreated with 20 μM of CQ for 24 or 48 h before incubation with 0.1 μCi of [14C]Asp.

In Vitro Tumor Cell–Fibroblast 3D Coculture. MiaPaca2-GFP cells (1 × 10³) were plated in U-bottom black-walled 96-well plates (Corning). After 48 h, 8 × 10³ primary fibroblasts were added (day 0); 72 h later, spheroids were formed, and treatment was initiated. Daily fluorescence readings were taken using a blue optical kit (Ex 490 nm/Em 510–570 nm) on a Modulus II Microplate Multimode Reader. Images were taken using a CX41 inverted microscope with a DP26 digital camera (Olympus).

Animal Studies. All reported animal studies were approved by the UCLA animal research review board. Four- to 6-wk-old male NSG mice were injected s.c. on bilateral flanks with 1 million MiaPaca2 or Miapaca2/SLC1A3 cells. Six- to 10-wk-old C57BL/6 female mice were injected s.c. on bilateral flanks with 5 × 10⁵ KPC cells. CQ was suspended in distilled water. VE-822 was suspended in tocophersolan. Both drugs were delivered orally at 60 mg/kg three times per week for 2 wk. Syngeneic mice with KPC tumors were killed when tumors reached 400 mm³ because at that size tumors began ulcerating.

1. Siegel RL, Miller KD, Jemal A (2017) Cancer statistics, 2017. *CA Cancer J Clin* 67:7–30.
2. Provenzano PP, et al. (2012) Enzymatic targeting of the stroma ablates physical barriers to treatment of pancreatic ductal adenocarcinoma. *Cancer Cell* 21:418–429.
3. Perera RM, et al. (2015) Transcriptional control of autophagy-lysosome function drives pancreatic cancer metabolism. *Nature* 524:361–365.
4. Yang S, et al. (2011) Pancreatic cancers require autophagy for tumor growth. *Genes Dev* 25:717–729.
5. Kamphorst JJ, et al. (2015) Human pancreatic cancer tumors are nutrient poor and tumor cells actively scavenge extracellular protein. *Cancer Res* 75:544–553.
6. Commisso C, et al. (2013) Macropinocytosis of protein is an amino acid supply route in Ras-transformed cells. *Nature* 497:633–637.
7. Davidson SM, Vander Heiden MG (2017) Critical functions of the lysosome in cancer biology. *Annu Rev Pharmacol Toxicol* 57:481–507.
8. Rosenfeldt MT, et al. (2013) p53 status determines the role of autophagy in pancreatic tumour development. *Nature* 504:296–300.
9. Mukubou H, Tsujimura T, Sasaki R, Ku Y (2010) The role of autophagy in the treatment of pancreatic cancer with gemcitabine and ionizing radiation. *Int J Oncol* 37:821–828.
10. Donadelli M, et al. (2011) Gemcitabine/cannabinoid combination triggers autophagy in pancreatic cancer cells through a ROS-mediated mechanism. *Cell Death Dis* 2:e152.
11. Fu Z, et al. (2018) CQ sensitizes human pancreatic cancer cells to gemcitabine through the lysosomal apoptotic pathway via reactive oxygen species. *Mol Oncol* 12:529–544.
12. Fujii S, et al. (2008) Autophagy is activated in pancreatic cancer cells and correlates with poor patient outcome. *Cancer Sci* 99:1813–1819.
13. Strohecker AM, White E (2014) Autophagy promotes BrafV600E-driven lung tumorigenesis by preserving mitochondrial metabolism. *Autophagy* 10:384–385.
14. Guo JY, et al. (2016) Autophagy provides metabolic substrates to maintain energy charge and nucleotide pools in Ras-driven lung cancer cells. *Genes Dev* 30:1704–1717.
15. Singh R, et al. (2009) Autophagy regulates lipid metabolism. *Nature* 458:1131–1135.
16. Hamer I, Van Beersel G, Arnould T, Jadot M (2012) Lipids and lysosomes. *Curr Drug Metab* 13:1371–1387.
17. Kamphorst JJ, et al. (2013) Hypoxic and Ras-transformed cells support growth by scavenging unsaturated fatty acids from lysophospholipids. *Proc Natl Acad Sci USA* 110:8882–8887.
18. Fujiwara Y, Wada K, Kabuta T (2017) Lysosomal degradation of intracellular nucleic acids-multiple autophagic pathways. *J Biochem* 161:145–154.
19. Weber G, et al. (1991) Regulation of de novo and salvage pathways in chemotherapy. *Adv Enzyme Regul* 31:45–67.
20. Aird KM, Zhang R (2015) Nucleotide metabolism, oncogene-induced senescence and cancer. *Cancer Lett* 356:204–210.
21. Nathanson DA, et al. (2014) Co-targeting of convergent nucleotide biosynthetic pathways for leukemia eradication. *J Exp Med* 211:473–486.
22. Laks DR, et al. (2016) Inhibition of nucleotide synthesis targets brain tumor stem cells in a subset of glioblastoma. *Mol Cancer Ther* 15:1271–1278.
23. Le TM, et al. (2017) ATR inhibition facilitates targeting of leukemia dependence on convergent nucleotide biosynthetic pathways. *Nat Commun* 8:241.
24. Livesey KM, Tang D, Zeh HJ, Lotze MT (2009) Autophagy inhibition in combination cancer treatment. *Curr Opin Investig Drugs* 10:1269–1279.
25. Piao S, Amaravadi RK (2016) Targeting the lysosome in cancer. *Ann N Y Acad Sci* 1371:45–54.
26. Wolpin BM, et al. (2014) Phase II and pharmacodynamic study of autophagy inhibition using hydroxychloroquine in patients with metastatic pancreatic adenocarcinoma. *Oncologist* 19:637–638.
27. Boone BA, et al. (2015) Safety and biologic response of pre-operative autophagy inhibition in combination with gemcitabine in patients with pancreatic adenocarcinoma. *Ann Surg Oncol* 22:4402–4410.
28. Fokas E, et al. (2012) Targeting ATR in vivo using the novel inhibitor VE-822 results in selective sensitization of pancreatic tumors to radiation. *Cell Death Dis* 3:e441.
29. Zeman MK, Cimprich KA (2014) Causes and consequences of replication stress. *Nat Cell Biol* 16:2–9.
30. Poli J, et al. (2012) dNTP pools determine fork progression and origin usage under replication stress. *EMBO J* 31:883–894.
31. Bester AC, et al. (2011) Nucleotide deficiency promotes genomic instability in early stages of cancer development. *Cell* 145:435–446.
32. Xu YZ, Huang P, Plunkett W (1995) Functional compartmentation of dCTP pools. Preferential utilization of salvaged deoxycytidine for DNA repair in human lymphoblasts. *J Biol Chem* 270:631–637.
33. Hosios AM, et al. (2016) Amino acids rather than glucose account for the majority of cell mass in proliferating mammalian cells. *Dev Cell* 36:540–549.
34. Birsoy K, et al. (2015) An essential role of the mitochondrial electron transport chain in cell proliferation is to enable aspartate synthesis. *Cell* 162:540–551.
35. Leal AM, de Queiroz JD, de Medeiros SR, Lima TK, Agnez-Lima LF (2015) Violacein induces cell death by triggering mitochondrial membrane hyperpolarization in vitro. *BMC Microbiol* 15:115.
36. Feig C, et al. (2012) The pancreas cancer microenvironment. *Clin Cancer Res* 18:4266–4276.
37. Vonlaufen A, et al. (2008) Pancreatic stellate cells: Partners in crime with pancreatic cancer cells. *Cancer Res* 68:2085–2093.
38. Toste PA, et al. (2016) Chemotherapy-induced inflammatory gene signature and protumorigenic phenotype in pancreatic CAFs via stress-associated MAPK. *Mol Cancer Res* 14:437–447.
39. Garcia-Bermudez J, et al. (2018) Aspartate is a limiting metabolite for cancer cell proliferation under hypoxia and in tumours. *Nat Cell Biol* 20:775–781.
40. Raben N, Puertollano R (2016) TFEB and TFE3: Linking lysosomes to cellular adaptation to stress. *Annu Rev Cell Dev Biol* 32:255–278.
41. Zhang N, et al. (2018) Increased amino acid uptake supports autophagy-deficient cell survival upon glutamine deprivation. *Cell Rep* 23:3006–3020.
42. Son J, et al. (2013) Glutamine supports pancreatic cancer growth through a KRAS-regulated metabolic pathway. *Nature* 496:101–105.
43. Abu-Remaileh M, et al. (2017) Lysosomal metabolomics reveals V-ATPase- and mTOR-dependent regulation of amino acid efflux from lysosomes. *Science* 358:807–813.
44. Massey AJ (2017) Modification of tumour cell metabolism modulates sensitivity to Chk1 inhibitor-induced DNA damage. *Sci Rep* 7:40778.
45. Liu EY, et al. (2015) Loss of autophagy causes a synthetic lethal deficiency in DNA repair. *Proc Natl Acad Sci USA* 112:773–778.
46. Bachem MG, et al. (2005) Pancreatic carcinoma cells induce fibrosis by stimulating proliferation and matrix synthesis of stellate cells. *Gastroenterology* 128:907–921.
47. Kadera BE, et al. (2013) MicroRNA-21 in pancreatic ductal adenocarcinoma tumor-associated fibroblasts promotes metastasis. *PLoS One* 8:e71978.

CELL BIOLOGY